

# Distribution features of four-port by reflective covered grating

JINHAI HUANG, BO WANG\*, XU YANG, LINJIAN HUANG, WEIYI YU, JIAHAO LI, XIAOFENG WANG, HONG ZOU, LIQUN LIU, GUODING CHEN, QU WANG, LIANG LEI, LI LUO

*School of Physics and Optoelectronic Engineering, Guangdong University of Technology, Guangzhou 510006, China*

The four-port reflection splitter with 0th order suppressed is proposed.  $\text{HfO}_2$  was chosen as the material for the grating ridges, achieving a highly-efficient splitting effect. Under normal incidence at 1550 nm wavelength, efficiencies of  $\pm 1$  and  $\pm 2$  orders under TE polarization are 24.45% and 24.56%, respectively, which are 24.10% and 24.08% under TM polarization, respectively. The 0th order of both polarizations is less than 1%. The structure was studied using rigorous coupled-wave analysis and simulated annealing algorithm. In addition, the electric field map of the energy distribution inside the grating during diffraction was depicted by the finite element method.

(Received May 4, 2023; accepted October 9, 2023)

*Keywords:* Four-port splitter, Under normal incidence, Polarization independence

## 1. Introduction

In recent years, the optoelectronics industry has been developing rapidly, and the integration and precision of optoelectronic devices are becoming more and more important. Beam splitter [1-4] is an optical device based on diffraction principle, which can distribute the energy of incident light evenly to two or more channels. Due to its high resolution, compact structure and light weight, grating beam splitter plays an important role in many fields, such as optical sensors [5-7], optical communication [8-10], optical storage [11,12], laser processing [13,14] etc. With the development of grating diffraction theory and precision processing technology, various beam splitters with excellent performance and precise dimensions have been designed. Wang et al. proposed an efficient zero-order elimination two-port grating [15]. Shu et al. proposed a high-efficiency three-port encapsulated grating [16]. Xiang et al. proposed a single-slot, four-port grating with a total diffraction efficiency of 86% [17]. Gao et al. proposed a polarization-independent four-port grating with a total efficiency of 94.16% for TE polarization and 94.48% for TM polarization [18].

In this paper, we propose a high-efficiency reflective four-port encapsulated grating.  $\text{HfO}_2$  [19,20] is chosen as the material for the grating ridge, which is considered as an ideal material to replace  $\text{SiO}_2$  in the electronics industry, and it is an excellent transparent material in the visible to infrared range with low absorption and scattering losses of light waves, which is suitable for making high diffraction efficiency gratings. In addition, the grating designed in this paper is based on the vertical incidence of 1550 nm light wave, and  $\text{HfO}_2$  maintains a stable refractive index near this wavelength with a wide wavelength tolerance

bandwidth, which is of great significance for the practical application of gratings. In the design of grating structure parameters, we used rigorous coupled-wave analysis (RCWA) [21-23] and simulated annealing algorithm (SAA) [24,25]. The optimized grating has high diffraction efficiency and excellent uniformity, for TE polarization, the 0th order efficiency is 0.13%,  $\pm 1$ st orders efficiencies are 24.45%,  $\pm 2$ nd orders efficiencies are 24.56%, and the total efficiency is 98.15%, for TM polarization, the 0th order diffraction efficiency is 0.92%,  $\pm 1$ st orders efficiencies are 24.10%, and  $\pm 2$ nd orders efficiencies are 24.08%. The high diffraction efficiency and uniformity of both TE and TM polarization are maintained for the same grating structure parameters, indicating the polarization-independent nature of the grating. To ensure the accuracy of the data, we use finite element method (FEM) [26-28] to calculate the optimized grating diffraction efficiency and analyze the electric field map of the energy distribution inside the grating during the diffraction process.

## 2. Design principle and optimization

The two-dimensional and three-dimensional structure of the four-port encapsulated grating is shown in Fig. 1. As can be seen from Fig. 1, the grating consists of four layers: cover layer, grating layer, reflection layer, and grating substrate. The cover layer and grating substrate are composed of fused silica with refractive index of  $n_2=1.444$ , the grating ridge is made of  $\text{HfO}_2$  with refractive index of  $n_3=1.877$ , the medium of the grating groove is air with refractive index of  $n_1=1.0$ . The reflection layer is made of silver with refractive index of  $n_m=0.313-i*10.605$  [29,30].

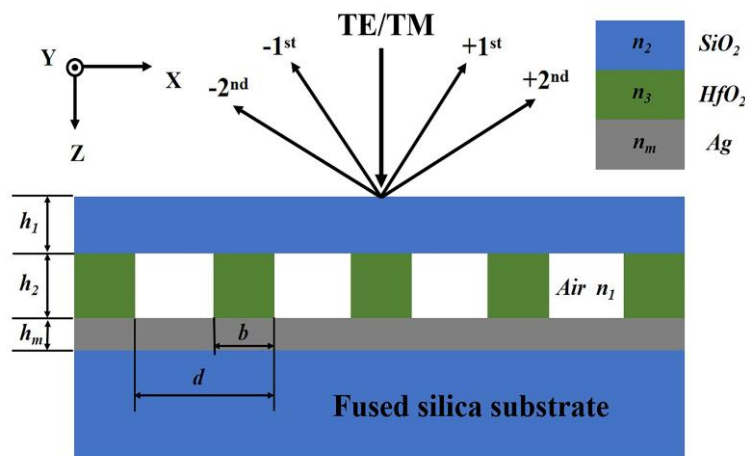
$h_1$  is the thickness of the cover layer,  $h_2$  is the height of the grating ridge,  $d$  is the grating period,  $b$  is the width of the grating ridge, and the duty cycle of the grating is  $f=b/d$ . Above the cover layer is the incident region consisting of air, and the incident wavelength of 1550 nm is incident vertically onto the upper surface of the grating, and the energy of the incident light is mainly diffracted to  $\pm 1$ st and  $\pm 2$ nd orders. Due to the symmetric structure of the grating, efficiencies of the positive and negative diffraction orders are equal under normal incidence, so only the transmission efficiencies of 0th, -1st and -2nd orders need to be calculated. RCWA is a very effective tool for dealing with electromagnetic field problems of periodic structures (especially diffraction gratings), and can effectively calculate the diffraction efficiency for different grating parameters. To obtain the optimal grating parameters, SAA is used in the solution space to find the global optimal solution randomly, the objective function of the SAA method is:

$$\varphi(d, h_1, h_2, f) = [1 - (\eta_{total} - |\eta_{-1} - \eta_{-2}|)], \quad (1)$$

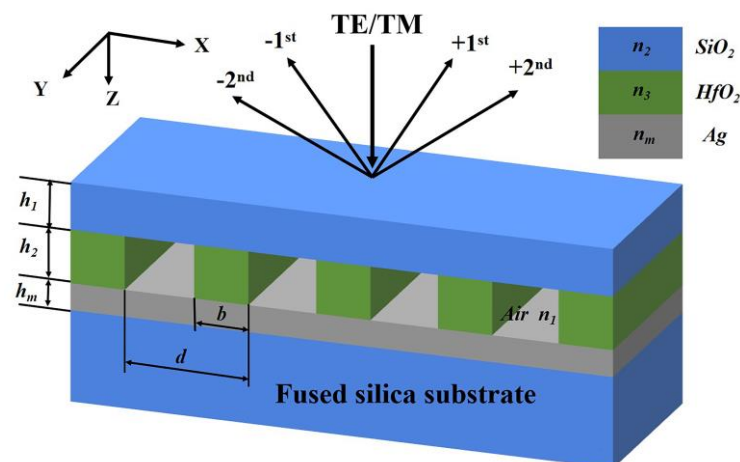
where  $\eta_{total}$  represents the sum of the diffraction efficiencies of the -1st and -2nd orders under a single polarization,  $\eta_{-1}$  represents the diffraction efficiency of the -1st order, and  $\eta_{-2}$  represents the diffraction efficiency of the -2nd order. From equation (1), it is known that the minimum value is obtained when the four-port grating has the optimal diffraction efficiency, while the optimal grating parameters ( $d, h_1, h_2, f$ ) can be obtained. In order to achieve the polarization-insensitive characteristic so that both TE and TM polarization have optimal diffraction efficiency for the same grating parameters, the objective function should be further expressed as:

$$\varphi = \frac{\varphi_{TE} + \varphi_{TM}}{2}, \quad (2)$$

where  $\varphi_{TE}$  and  $\varphi_{TM}$  represent the cost functions of TE polarization and TM polarization, respectively.



(a)



(b)

Fig. 1. Schematic of the four-port encapsulated grating with zeroth order suppressed under normal incidence: (a) 2-D view (b) 3-D view (color online)

Under the condition of vertical incidence of 1550 nm light wave, the optimal parameters of the grating ( $d, h_1, h_2, f$ ) are calculated as shown in Table 1, and the order diffraction efficiencies of the two polarizations under the optimal grating parameters are shown in Table 2. To ensure the accuracy of the optimization results, FEM was used to calculate the diffraction efficiency of the two polarizations under the optimal grating parameters, and the results are shown in Table 2. From Table 2, it can be seen that the diffraction efficiencies calculated by the two methods are almost the same, so the optimization results are credible.

Table 1. The optimal parameters of four-port transmission beam splitter grating with zeroth order suppressed

$\lambda$	$d$	$f$	$h_1$	$h_2$
1550 nm	4.617 $\mu\text{m}$	0.45	0.95 $\mu\text{m}$	1.41 $\mu\text{m}$

Table 2. Diffraction efficiency and uniformity of the grating obtained by the two methods, where  $\lambda=1550$  nm,  $d=4.617$   $\mu\text{m}$ ,  $f=0.45$ ,  $h_1=0.95$   $\mu\text{m}$ ,  $h_2=1.41$   $\mu\text{m}$

Polarization	0th	$\pm 1\text{st}$	$\pm 2\text{nd}$	U
TE (FEM)	0.13%	24.39%	24.58%	0.38%
TE (RCWA)	0.13%	24.45%	24.56%	0.22%
TM (FEM)	0.95%	24.00%	24.10%	0.21%
TM (RCWA)	0.92%	24.10%	24.08%	0.04%

The propagation of the incident light in the grating is affected by the thickness of the cover layer, and the height of the grating ridge directly affects the phase difference of

the coupled light waves. Fig. 2 shows the transmission efficiency of the four-port grating beam splitter as a function of the thickness of the cover layer and the height of the grating ridge. As can be seen in Fig. 2, when  $h_1=0.95$   $\mu\text{m}$  and  $h_2=1.41$   $\mu\text{m}$ , the polarization efficiencies of TE at 0th, -1th and -2nd orders are 0.13%, 24.46% and 24.56%, respectively, with a total efficiency of 98.15%, and at TM polarization conditions, the efficiencies at 0th, -1st and -2st orders are 0.92%, 24.10% and 24.08%, respectively, with a total efficiency of 97.28%. For the same grating structure, TE and TM polarization can output both high efficiency. In addition, the uniformity of the diffraction efficiency at each port is an important measure of the performance of the grating beam splitter. The uniformity of the output efficiency at each port can be described by U, as:

$$U = \frac{(\eta_{max} - \eta_{min})}{(\eta_{max} + \eta_{min})} \times 100\% , \quad (3)$$

where  $\eta_{max}$  and  $\eta_{min}$  are the maximum and minimum diffraction efficiencies for non-zero diffraction orders in the four-port beam splitter, respectively. The results obtained by calculating Eq. (3) are shown in Table 2, and the grating diffraction efficiency has excellent uniformity under both TE and TM polarizations. Compared with the previously mentioned references [17,18], the four-port grating beam splitter proposed in this paper has higher efficiency and better uniformity.

The influence of the reflective layer thickness on the diffraction efficiency of the grating has also been analyzed. Fig. 3 shows the relationship between the thickness of the reflective layer and the diffraction efficiency of each order, from which it can be seen that when the thickness of the reflective layer is 0.1  $\mu\text{m}$ , the diffraction efficiency of each order reaches its maximum value, and when the thickness of the reflective layer is greater than 0.1  $\mu\text{m}$ , the diffraction efficiency no longer changes. Considering the cost factor in practical application, the thickness of the reflective layer is set to 0.1  $\mu\text{m}$  in this paper.

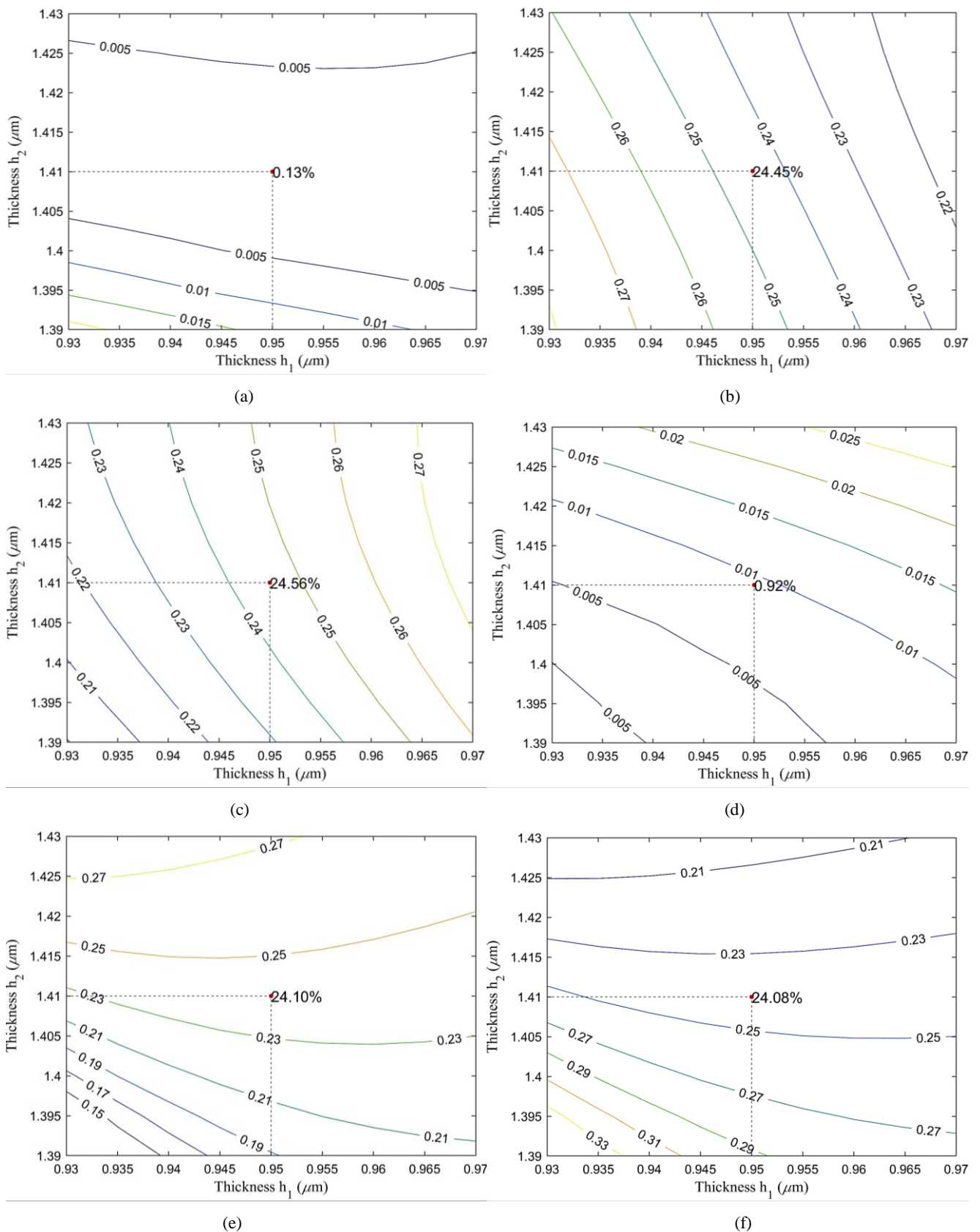


Fig. 2. Efficiencies in orders for the grating versus thicknesses of the covering layer and the grating ridge under normal incidence with  $\lambda=1550$  nm, period  $d=4.617$   $\mu\text{m}$ , and duty cycle  $f=0.45$ : (a) 0th order of TE polarization, (b)  $\pm 1$ st orders of TE polarization, (c)  $\pm 2$ nd orders of TE polarization, (d) 0th order of TM polarization, (e)  $\pm 1$ st orders of TM polarization, (f)  $\pm 2$ nd orders of TM polarization (color online)

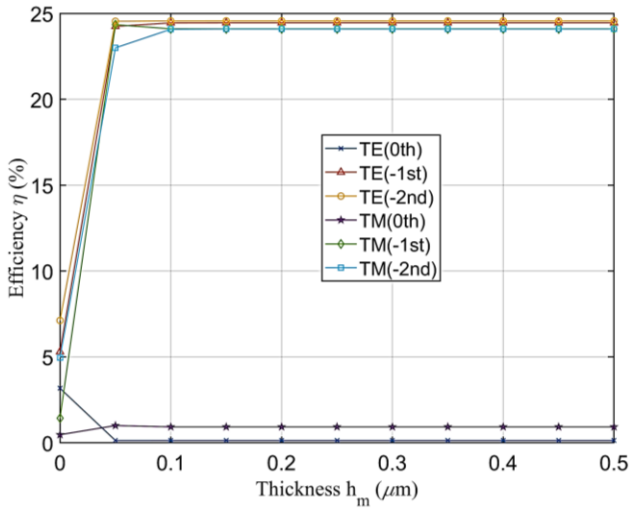


Fig. 3. The efficiency corresponding to the thickness of the reflector under normal incidence: TE polarization and TM polarization, where  $f=0.45$ ,  $h_1=0.95 \mu\text{m}$  and  $h_2=1.41 \mu\text{m}$  (color online)

In addition, the physical mechanism of grating diffraction is explained by the finite element method based on the grating structure parameters obtained from RCWA optimization, and the optimization results of RCWA are verified. Table 2 shows the comparison of the grating efficiency calculated by RCWA and FEM for the same grating parameters, and the results obtained by both methods are almost the same, so the data in this paper can be considered reliable. Fig. 3 shows the normalized electric field distribution and magnetic field distribution of the four-port reflective grating under the effect of two polarizations. It is obvious that under the condition of normal incidence, the incident light with a wavelength of 1550 nm propagates from the air to the top of the Ag reflector layer, and the energy of the light wave is effectively reflected back, and the energy distribution can hardly be found on the substrate.

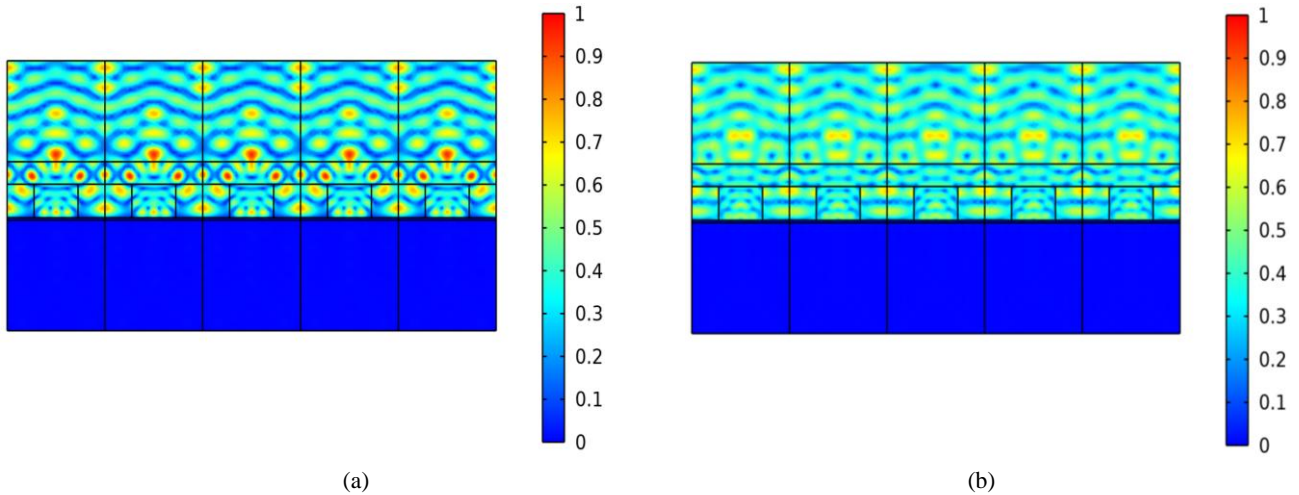


Fig. 4. The normalized electric field distribution with  $\lambda=1550 \text{ nm}$ ,  $d=4.617 \mu\text{m}$ ,  $f=0.45$ ,  $h_1=0.95 \mu\text{m}$ ,  $h_2=1.41 \mu\text{m}$ : (a) TE polarization and (b) TM polarization (color online)

### 3. Analysis and discussions

It is assumed that the light wave with a wavelength of 1550 nm will be incident vertically when the grating parameters are optimized. It is necessary to consider the impact of the deviation of incident wavelength and incident angle on the performance of the grating, as in reality, the wavelength of incident light always changes, and it cannot be guaranteed that the light is incident vertically. Fig. 4 depicts the relationship between the diffraction efficiency of the grating and the incident wavelength; It indicates that for TE polarization, the diffraction efficiency of the first and second orders is still higher than 20% when the incident wavelength is between 1540 and 1558 nm. In addition, for TM polarization, the

diffraction efficiency of the first and second orders is still higher than 20% when the incident wavelength is between 1545 and 1553 nm. Within the bandwidth range of the incident wavelength mentioned above, the 0th order diffraction efficiency of TE polarization and TM polarization are both lower than 3%. The results indicate that the four-port diffraction grating still has good performance within the aforementioned wavelength bandwidth range, and TE polarization has a wider bandwidth than TM polarization.

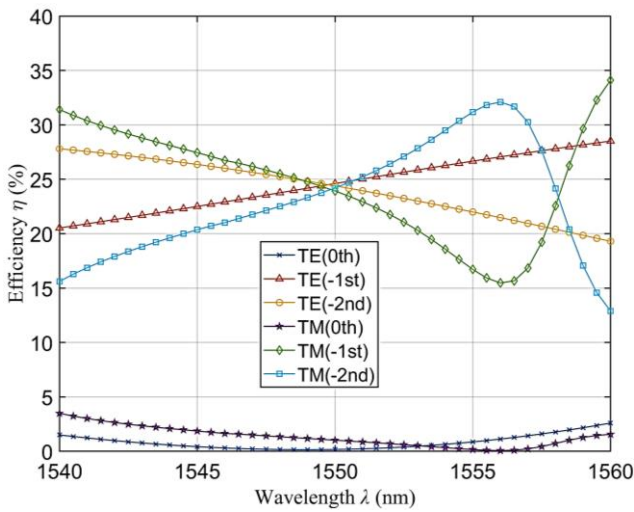
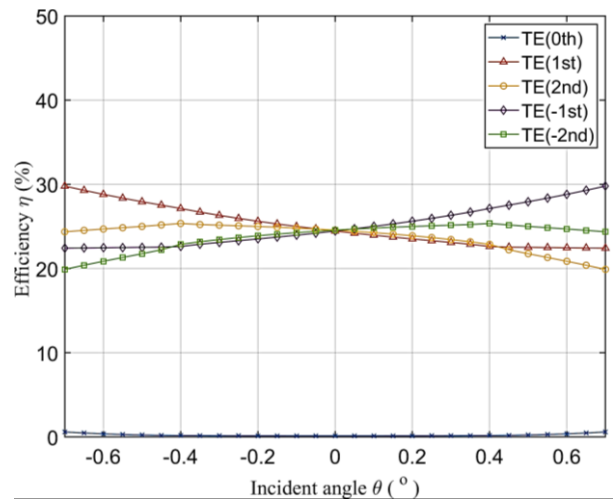


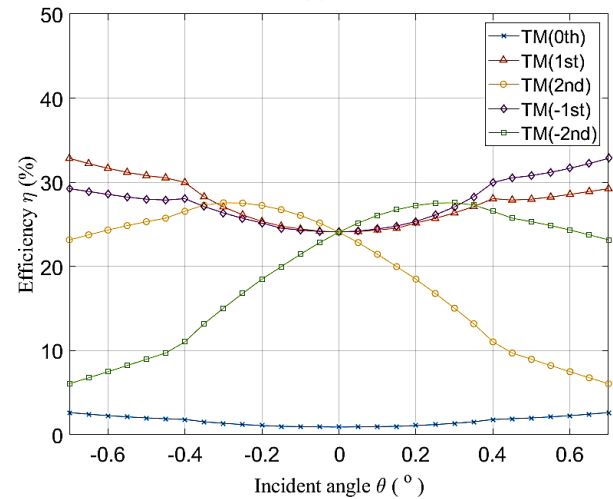
Fig. 5. The efficiency corresponding to the incident wavelength for both TE and TM polarizations under normal incidence, where  $d=4.617 \mu\text{m}$ ,  $f=0.45$ ,  $h_1=0.95 \mu\text{m}$  and  $h_2=1.41 \mu\text{m}$  (color online)

Fig. 5 shows the diffraction efficiency of the grating as a function of the incident angle. When the efficiency of the non-zero diffraction orders is required to be higher than 20%, the incident angle needs to be in the range of  $-0.6^\circ$  to  $0.6^\circ$  for TE polarization and  $-0.15^\circ$  to  $0.15^\circ$  for TM polarization. The 0th order diffraction efficiency is less than 3% for both TE and TM polarization over the bandwidth range. This indicates that the grating maintains high diffraction efficiency and 0th order rejection performance over the above incidence angle range.

Additionally, due to the influence of the processing process, the grating invariably experiences size deviations during the actual processing and preparation, so it's important to examine the impact of the grating structure parameters on the efficiencies of the grating diffraction. In Fig. 6, the diffraction efficiencies of the TE and TM polarization is plotted against the grating period. It can be seen that when the grating period  $d=4617 \text{ nm}$ , the diffraction efficiencies of the grating is optimal, in addition, for TE polarization, when the grating period is in the range of 4580-4667 nm, the diffraction efficiencies of -1st and -2nd orders are still higher than 20%, and for TM polarization, the diffraction efficiencies of -1st and -2nd orders are still higher than 20% when the grating period is in the range of 4604 -4634 nm. Fig. 7 shows the effect of grating duty cycle variation on the diffraction efficiency of TE and TM polarization levels, and it is easy to see that the grating has the best diffraction efficiency when the duty cycle  $f=0.45$ , and the -1st and -2nd orders diffraction efficiencies of TE and TM polarizations still exceed 20% when the duty cycle is in the range of 0.44-0.47. Within the bandwidth range discussed above, the 0th order diffraction efficiency of TE and TM polarization is less than 3%. The above results show that the period and duty cycle of the grating have good process tolerances and are of great importance for practical production.



(a)



(b)

Fig. 6. The diffraction efficiency corresponding to the incident angle for the incident wavelength of 1550 nm with the optimized grating profile parameters: (a) TE polarization and (b) TM polarization, where  $d=4.617 \mu\text{m}$ ,  $f=0.45$ ,  $h_1=0.95 \mu\text{m}$  and  $h_2=1.41 \mu\text{m}$  (color online)

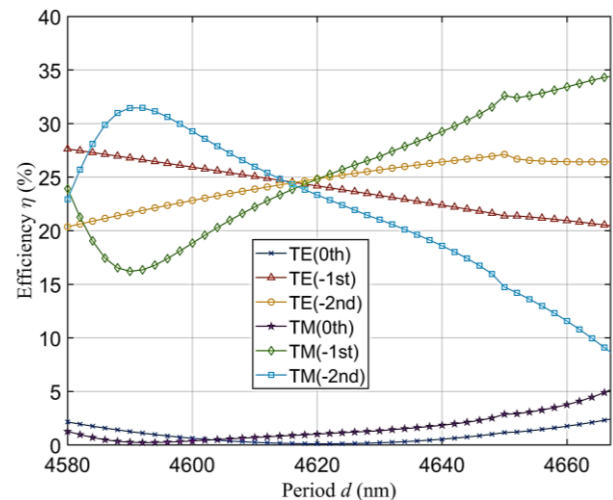


Fig. 7. The efficiency corresponding to the period under normal incidence: TE polarization and TM polarization, where  $f=0.45$ ,  $h_1=0.95 \mu\text{m}$  and  $h_2=1.41 \mu\text{m}$  (color online)

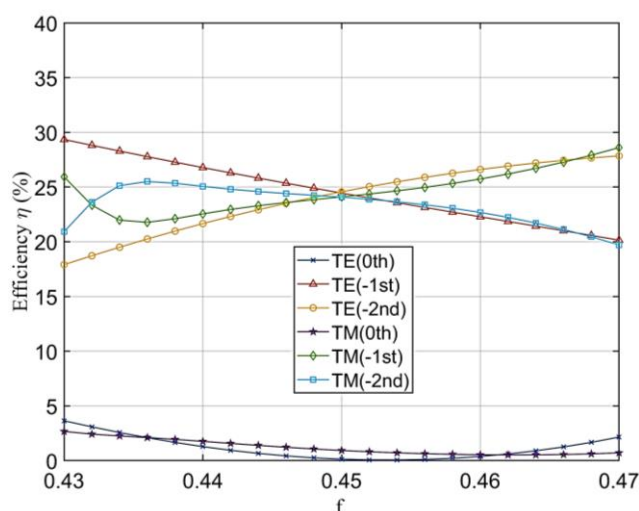


Fig. 8. The efficiency corresponding to duty cycle under normal incidence: TE polarization and TM polarization, where  $d = 4.617 \mu\text{m}$ ,  $h_1 = 0.95 \mu\text{m}$  and  $h_2 = 1.41 \mu\text{m}$  (color online)

#### 4. Conclusion

In this paper, a reflective four-port encapsulated grating beam splitter with 0th order rejection characteristics is proposed, and the optimized parameters of the grating are obtained by RCWA calculation and FEM verification with satisfactory results. For TE polarization, the  $\pm 1\text{st}$  orders efficiencies are 24.45% and  $\pm 2\text{nd}$  orders efficiencies are 24.56%, and for TM polarization, the  $\pm 1\text{st}$  orders efficiencies are 24.10% and  $\pm 2\text{nd}$  orders efficiencies are 24.08%, while the 0th order diffraction efficiencies for TE and TM polarization are close to zero. In addition, the effects of grating structure parameters, incident wavelength and incident angle on the grating performance are also analyzed considering practical applications, the results indicate that the grating has good process tolerance. The grating has not only polarization-independent performance, but also high diffraction efficiency and excellent uniformity, which are advantageous in the field of beam splitters.

#### Acknowledgements

This work is supported by the Science and Technology Program of Guangzhou (202002030284).

#### References

- [1] D. Mansouri, B. Rezaie, N. A. Ranjbar, A. Daeichian, *Eur. Phys. J. Plus* **137**(9), 1032 (2022).
- [2] T. Qiu, H. Ma, P. Xin, X. Zhao, Q. Liu, L. Chen, Y. Feng, Z. Yu, *Eur. Phys. J. Plus* **137**(1), 126 (2022).
- [3] R. Arunkumar, J. K. Jayabarathan, S. Robinson, *J. Optoelectron. Adv. M.* **21**(7-8), 435 (2019).
- [4] C. Gao, B. Wang, C. Fu, J. Fang, K. Wen, Z. Meng, Z. Nie, X. Xing, L. Chen, L. Lei, J. Zhou, *Opt. Commun.* **459**, 125063 (2020).
- [5] A. Shadab, S. K. Raghuvanshi, S. Kumar, *IEEE Sen. J.* **22**, 15650 (2022).
- [6] H. Wang, Z. Fu, Z. Ni, X. Zhang, C. Zhao, S. Jin, J. Jing, *Opt. Express* **29**(7), 11194 (2021).
- [7] S. Zhang, Y. Bi, L. Sun, Y. Chen, *IEEE Access* **9**, 41168 (2021).
- [8] Z. L. Hussain, R. S. Fyath, *Optik* **264**, 169456 (2022).
- [9] N. Jellali, M. Ferchichi, M. Najjar, *Optik* **244**, 166188 (2021).
- [10] S. Kumar, S. Rathee, P. Arora, D. Sharma, *J. Opt. Commun.* **43**(4), 585 (2022).
- [11] X. Tian, Y. Wang, Q. Zhao, Y. Li, H. Li, J. Qu, D. Zhong, Q. Jiaojiao, Z. Dongbin, *Optik* **248**, 168054 (2021).
- [12] X. Sun, Z. Zhang, Z. Sun, J. Zheng, X. Liu, H. Xia, *Macromol. Rapid Commun.* **43**, 2100863 (2022).
- [13] S. Shuai, G. Zhang, W. Shi, Z. Tian, Q. Sheng, Y. Zhang, H. Zhang, J. Yao, *Appl. Opt.* **58**(11) 2828 (2019).
- [14] W. He, Y. Liu, Z. Luo, X. Chen, G. Hu, C. Zhu, L. Zhu, *Optoelectron. Adv. Mat.* **16**(9-10), 391 (2022).
- [15] B. Wang, *IEEE Photon. J.* **8**(1), 2527706 (2016).
- [16] W. Shu, B. Wang, H. Li, L. Lei, L. Chen, J. Zhou, *Mod. Phys. Lett. B* **30**(06), 1650070 (2016).
- [17] C. Xiang, C. Zhou, W. Jia, J. Wang, *Proc. SPIE* **10818**, 1081812 (2018).
- [18] C. Gao, B. Wang, *Laser Phys.* **30**, 026203 (2020).
- [19] X. Liu, J. Zheng, Z. Xu, W. Du, Y. Zuo, H. Guo, W. Jing, H. Feng, *Opt. Mat.* **131**, 112641 (2022).
- [20] N. Sekar, *Opt. Mater.* **134**, 113073 (2022).
- [21] Z. Lin, B. Wang, K. Wen, *Opt. Commun.* **505**, 127499 (2022).
- [22] H. Wang, F. Zhang, C. Wang, J. Duan, *Opt. Laser Technol.* **149**, 107931 (2022).
- [23] M. G. Moharam, D. A. Pommet, E. B. Grann, T. K. Gaylord, *J. Opt. Soc. Am. A* **12**(5), 1077 (1995).
- [24] W. Liu, D. Jin, W. Shi, J. Cao, *Opt. Laser Technol.* **149**, 107878 (2022).
- [25] Z. Huang, B. Wang, *Opt. Laser Technol.* **152**, 108102 (2022).
- [26] H. Zhao, Z. Liu, C. Yu, C. Liu, Y. Zhan, *Opt. Laser Technol.* **152**, 108146 (2022).
- [27] F. A. Khatir, M. H. Sadeghi, S. Akar, *Opt. Laser Technol.* **147**, 107623 (2022).
- [28] I. Sakaev, J. Linden, A. A. Ishaaya, *Opt. Laser Technol.* **150**, 107938 (2022).
- [29] A. Ciesielski, L. Skowronski, M. Trzcinski, T. Szoplak, *Appl. Surf. Sci.* **421**, 349 (2017).
- [30] Z. Yin, Y. Lu, J. Yu, C. Zhou, *Chin. Opt. Lett.* **18**, 070501 (2020).

\*Corresponding author: wangb\_wsx@yeah.net